Modelling dynamic deformation of clay backing in ballistic impact of armour

Timothy G Zhang, Sikhanda S Satapathy

US Army Research Laboratory, Aberdeen Proving Ground, MD 21005, U.S.A.

timothy.g.zhang.civ@mail.mil

Abstract. In this study, a numerical model was developed to model the ballistic impact on an armour composed of ceramics, an Ultra-high-molecular-weight-polyethylene (UHMWPE) plate, and soft shoot-pack with clay backing. A material model, calibrated with experimental data from impact and drop-tests in clay blocks that accounted for the deformation rebound was used to model the clay. The numerical model captured the back face deformation of the armour system consisting of ceramics, composite, fabric, and the interactions with the clay backing. Ballistic impact tests were conducted in two sizes of clay blocks: 0.15 m cylindrical clay block contained in a polyvinyl chloride (PVC) pipe, and a 0.61 m by 0.61 m rectangular clay block contained in a metal frame. Repeated tests were conducted for three different armour thicknesses. The model results were found to be in very good agreement with the experimentally measured final clay deformation for both clay blocks and various armour thicknesses. The quantification of the peak dynamic clay deformation from the simulation and correlating it to residual clay deformation provides more insight into energy and momentum transmission behind armour.

1. INTRODUCTION

Current personal protective equipment (PPE) have drastically reduced battlefield fatalities by using high performance materials, such as Ultra-high-molecular-weight-polyethylene (UHMWPE) and ceramics, to defeat threats. Even when an armour defeats the projectile, impact load is still transferred to the body through the deforming back face of the armour. Roma Plastilina No.1 clay is typically used to characterize the load transfer from the deforming back face of the armour to the human body. Measurement of the residual clay deformation is used to represent the peak armour deformation.

However, the residual clay deformation can often be less than the peak dynamic clay deformation. In [1], ballistic impact tests were conducted to measure the indent depth in the clay backing. X-ray results showed that the clay rebounded after reaching the peak deformation. However, the qualities of X-ray images drop as the clay size increases and introduce errors for the measured dynamic clay indents. To correlate the dynamic to residual clay indents, a numerical approach would be desired.

A clay model was previously calibrated with experimental data from low velocity impact and drop tests [2]. However, there was no rebound in the clay under those impact conditions, or, only residual clay indents were measured; therefore the calibrated model did not account for the rebound. The clay rebound was also observed in the ballistic impact tests at various velocities and drop tests in [3].

In this study, ballistic impact tests were conducted in hard-armour and shoot-pack with clay backing. Three different thicknesses of hard-armour were used to investigate the effect of armour thickness on the clay indent. Two sizes of clay block were used as the backing to study the effect of clay size on the clay deformation response, especially the dynamic deformation vs the residual deformation. The Finite Element models were developed to simulate the ballistic response of the ceramics, hard-armour, shoot-pack, clay backing and their interaction. The clay model developed in [2] was re-calibrated to account for rebound using the test data in [3]. The residual clay indents from the ballistic impact tests of various armour thicknesses and clay sizes were used to validate the model.

2. EXPERIMENTS

Ballistic impact tests were performed on ceramic/composite targets with a clay backing to characterize the back-face response of the armour material. The 0.10 m (4 inch) × 0.10 m ceramic and 0.20 m (8 inch) × 0.20 m composite layer were bonded together. A 0.20 m (8 inch) × 0.20 m shoot-pack layer was placed behind the composite layer and was backed by a clay-block. The test configurations are shown in Figure 1. Two configurations of the clay backing were used, as shown in Figure 2: 1) 0.15 m (6 inch) diameter × 0.28 m (11 inch) thick cylindrical clay block contained in a polyvinyl chloride (PVC) pipe with a 0.03 m (1 inch) thick plywood backing at the distal end of impact, and 2) 0.61 m (2 ft) × 0.61 m × 0.14 m (5.5 inch) thick rectangular clay block contained in a metal container with 0.02 m (3/4 inch) thick plywood in the back. The clay–pipe configuration was used to capture the dynamic deformation of the clay. Due

https://doi.org/10.52202/078352-0038

to the smaller size of clay and the confinement of PVC, the clay response is likely to be affected by the boundary conditions at earlier time. The larger rectangular clay block configuration was used to obtain the relationship between the areal density of armour and the clay residual indents.

In the experiments, a steel core projectile impacted the centres of the ceramic plates at constant velocity. Three thicknesses of hard-armour were used in the tests. The areal densities of the hard-armour were 31.2 kg/m^2 (6.4 psf), 35.1 kg/m^2 (7.2 psf), and 39.0 kg/m^2 (8.0 psf), the first and second were 80% and 90% of the third one. The thickness ratio of the ceramic plate to composite plate was fixed for the three different thickness armours. In order for the composite plates to glide along rods, holes, which were slighter larger than the rod size, were drilled at the four corners of the composite plates and rods were inserted in to the holes.

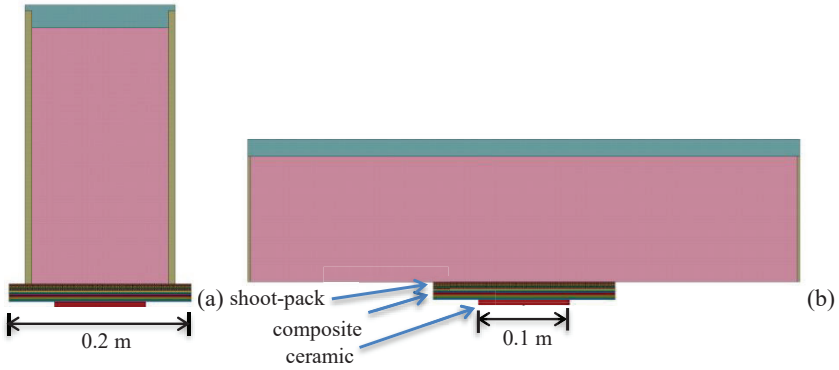

Figure 1 Impact of a hard armour and shoot-pack, with (a) 0.15 m diameter cylindrical clay backing, and (b) 0.61 m × 0.61 m rectangular clay backing (half model)

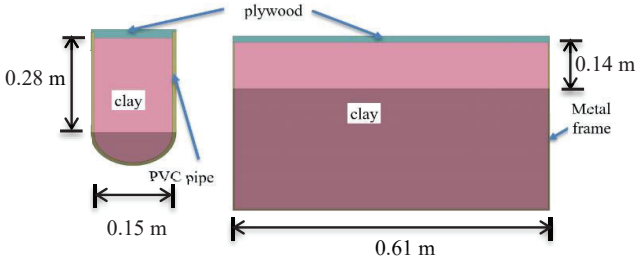

Figure 2 (a) 0.15 m diameter clay block, and (b) 0.61 m × 0.61 m clay block (half model)

Figure 3 shows the normalized residual clay indents measured after the impact tests for both 0.15 m and 0.61 m clay block. The clay indent was normalized by the maximum indent of all the test data. The test data was scattered, especially for the case of 0.15 m clay block. The response of smaller clay was more likely to be affected by the boundary conditions from the PVC pipe. As expected, the clay indents decreased with increase in the armour areal density. For thicker hard-armour, less energy of the projectile was transferred to the shoot-pack and subsequently to the clay block. The residual clay indents were higher in the larger clay blocks since the clay can continue to deform for longer period of time before the boundary conditions affected the deformation.

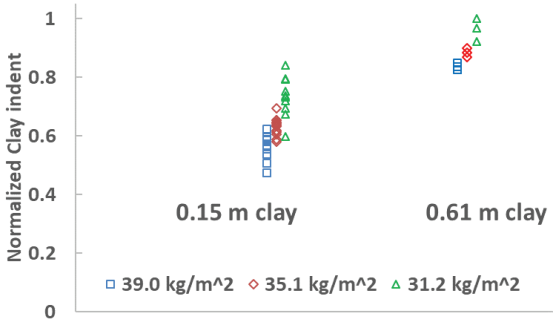

Figure 3 Normalized residual clay indents for 0.15 m and 0.61 m clay block for 39.0, 35.1 and 31.2 kg/m^2 hard-armour

https://doi.org/10.52202/078352-0038

3. FINITE ELEMENT MODELS

Figure 4 shows a schematic of the computational model of 0.61 m × 0.61 m clay block used in the study. The ceramic plate was bonded to a composite plate backed by the shoot-pack, which rested on Roma Plastilina No.1 clay backing. The clay was contained in a metal container with 0.02 m thick plywood in the back. The commercial software, LS-DYNA was used to compute the ballistic interaction between the bullet, armour and the clay block. The geometry was symmetric with respect to orthogonal mid-planes; hence a quarter symmetry model could be used for efficiency. However, as soon as the ceramic material cracks, the random fracture destroy the symmetry, and hence a full model should be used. We used a half symmetry model with symmetric boundary conditions as a compromise between efficiency and accuracy. Holes were created at the corners of the composite plate and the nodes at the hole edges were only allowed to move along impact direction to represent the gliding motion along the rods. A rigid wall boundary condition was used at the plywood location.

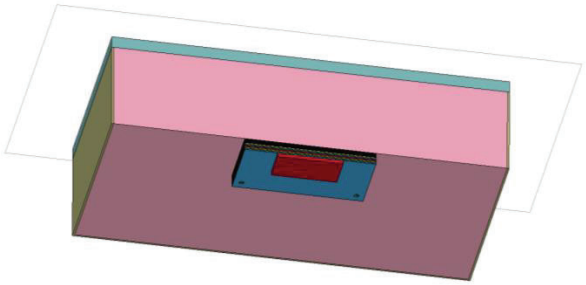

Figure 4 Computational model for the hard-armour, shoot-pack and 0.61 m clay block (half model)

The material models for the composite, shoot-pack and clay were calibrated with impact test data, while the material models for the bullet, ceramics, metal frame, PVC pipe and plywood were obtained from the literature or material library from EPIC code [7]. The final clay indent data were used to validate the computational model.

3.1 UHMWPE panels

The UHMWPE composite was made of 0/90º plies of unidirectional laminate sheets. To accurately model the failure in vicinity of the contact areas, a finer mesh was used near the point of impact, whereas a coarser mesh was used elsewhere. An example of the mesh for one layer is shown in Figure 5 (only a quarter model is shown).

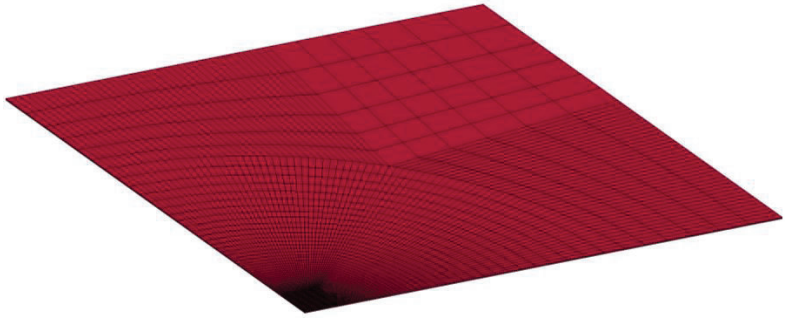

Figure 5 Mesh for one layer of UHMWPE composite (quarter model)

A numerical model was developed and characterized for UHMWPE [4], which was used in this analysis. In that model *MAT62, only fibre tension-shear failure and fibre crush failure were included. In addition, the delamination failure was explicitly modelled using tie-break contact between adjacent composite layers. The material model was characterized with a series of ballistic experiments, including V_{50} data, back face deformation data, and delamination failure. The model captured the test data very well. The details for the model can be found in [4].

https://doi.org/10.52202/078352-0038

In the finite element model, a few laminates were fused into a single computational layer for computational efficiency. Ten "fused" layers were used for the 39.0 kg/m^2 (areal density) armour and the number of "fused" layers was proportional to the areal density. Two elements per layer were used along the thickness direction to account for bending effects. Eroding contact algorithm was used to delete failed material near the projectile impact site. Eroding contact algorithm is computationally expensive, and hence was used only in the zone near impact where material failure was expected.

3.2 Clay

A material model *MAT_PLASTICITY_COMPRESSION_TENSION [2] for the clay was developed based on quasi-static compression tests, drop tests and impact tests at medium rates. In the drop tests a 1 kg hemispherical nose cylindrical projectile was dropped from a height of 2 m on the clay block. In the impact tests, a 0.2 kg hemispherical nose projectile with a long tail impacted the clay block at impact velocity up to 55 m/s. The projectiles used in the drop and impact tests were shown in Figure 6. In the impact tests and drop tests, rectangular clay blocks of size 0.30 m × 0.30 m × 0.28 m thick was used, which doubled in thickness compared to the clay block used in this work. The rectangular clay block was placed on a table during the tests, which was modelled by using a rigid surface constraint boundary condition in the numerical model. The other sides were kept stress free. In the clay material model, compression and tension responses were treated differently. The strain rate effect was included in the model.


(a)
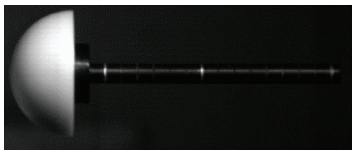
(b)

Figure 6 The projectile used in (a) drop test, and (b) impact test

However, there was no rebound in the clay of 55 m/s impact tests, and only residual clay indents were measured in the drop tests, therefore the calibrated model did not account for deformation rebound [2]. Additional tests were conducted at different impact velocities. Also the drop tests were repeated, and the time history of clay indents were recorded [3]. The deformation rebound was observed from the new test data and the clay model was therefore re-calibrated. Below the results of the new model are discussed.

The comparison between simulation and experimental results are shown in Figure 7 and Figure 8. The clay model captures the response including the rebound observed in the experiments. However, even though the calculated rebound is within the experimental error for the drop tests, the calculated rebound was slightly outside the experimental bounds for the impact tests. The peak clay indent was captured reasonably well in the calculation for various impact velocities.

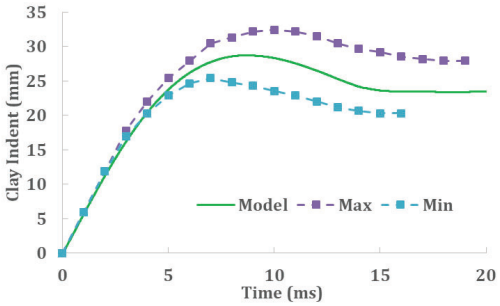

Figure 7 Comparison between model and drop tests

https://doi.org/10.52202/078352-0038

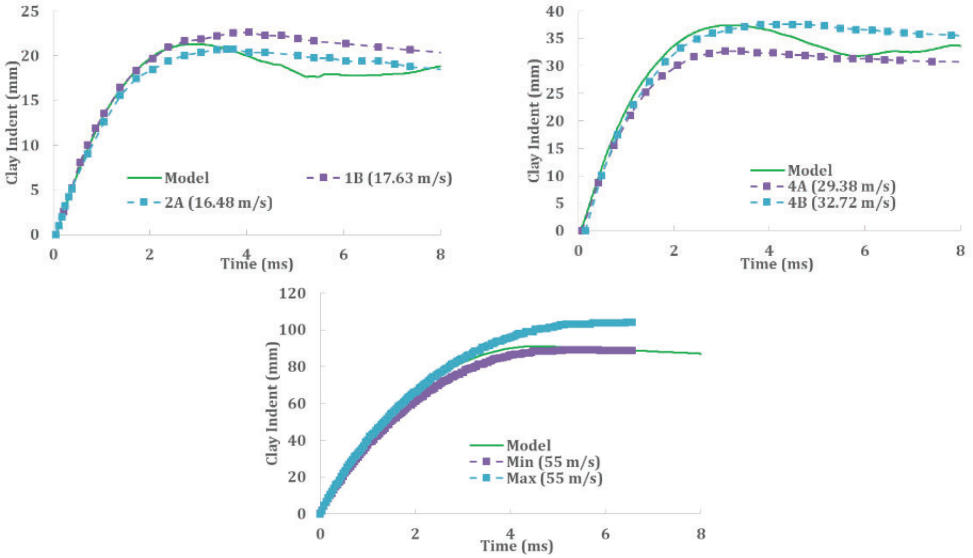

Figure 8 Comparison between model and impact tests

3.3 Shoot-pack

The shoot-pack model was developed previously [5]. The model is briefly described here. The woven structures of yarns were modelled. Due to interaction between yarns, the model was not computationally efficient. Figure 9 (a) shows the FE meshes for yarn model for one layer. Non-uniform meshes were used with finer meshes in the impact zone. Figure 9 (b) shows the meshes in the impact zone. Only a quarter of model was shown here.

The predicted time history of BFD from the yarn model had reasonable agreements with the test data [5]. The model had better accuracy since woven structures was captured in the model.

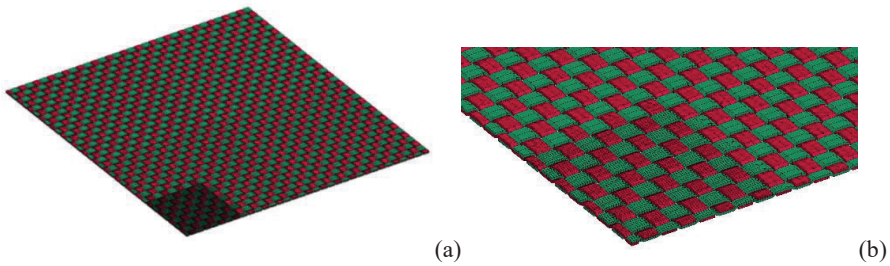

(a) (b)

Figure 9 FE meshes for (a) one layer of weft and warp yarns, and (b) yarn meshes in the impact zone (only a quarter model was shown)

3.4 Ceramics model

The JH-2 ceramics material model available in LS-DYNA was used for the SiC plate. This model tracks damage evolution and adjusts the material strength based on the amount of damage accumulation. The pressure is calculated using a prescribed equation of state. The material parameters for this model can be found in [6].

https://doi.org/10.52202/078352-0038

4. RESULTS

Figure 10 and Figure 11 show the comparisons between the simulation result and residual clay indents measured from the ballistic test on the armour backed by clay. The residual clay indent data are plotted next to end of the simulation time, which was ~2 ms for 0.15 m clay case and ~3.5 ms for 0.61 m clay case. The simulation end time was selected so that the clay deformations reach equilibrium (clay velocity was small). Overall, the calculations showed good agreement with the residual clay indents measured in the experiments. The 0.15 m diameter clay started to rebound at ~1 ms and the total rebound can be up to about 15% of the peak deformation. However, the 0.61 m × 0.61 m clay started to rebound at a later time ~1.5 ms and the rebound was much less pronounced compared to 0.15 m diameter clay case. The 0.61 m × 0.61 m clay continued to deform after the small rebound. The boundary conditions seem to affect the clay response. The final clay indent is less than the peak indent for 0.15 m diameter clay case, whereas the final clay indent is almost the same as the peak indent for 0.61 m × 0.61 m clay case.

The time history of the clay indents were similar for hard-armours of different thicknesses, including the time when the slope change at ~0.1 ms, time when the rebound occurs, and then subsequently the indent depth increases. The major differences are the magnitudes for different thickness armours.

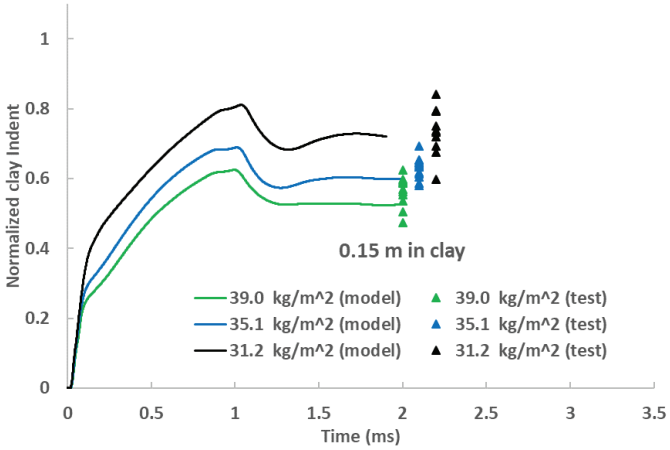

Figure 10 The time history of clay indent for 0.15 m diameter clay (test data is the residual clay indent measured after the impact tests)

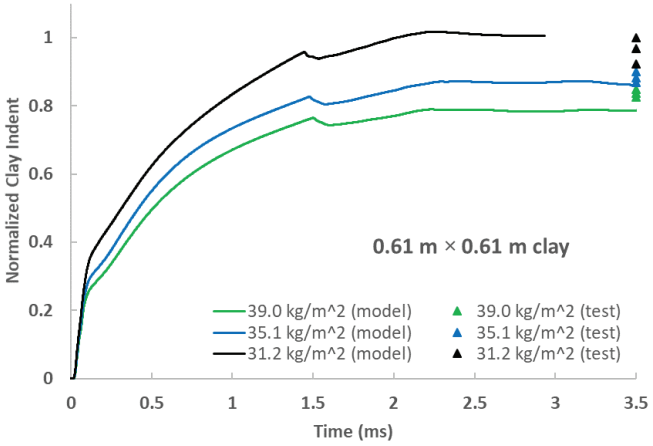

Figure 11 The time history of clay indent for 0.61 m × 0.61 m clay block (test data is the residual clay indent measured after the impact tests)

https://doi.org/10.52202/078352-0038

5. DISCUSSIONS

Figure 12 combines Figure 10 and Figure 11 to understand the effect of clay size on the clay deformation. The solid lines are the time histories of centre indents in 0.61 m clay blocks, and the dashed lines are for 0.15 m clay blocks. The clay deformations are observed to be almost identical until ~0.7 ms when the clay boundary conditions started to affect the response. The clay indent increases rapidly when the shoot-pack starts to deform. Around 0.1 ms the clay deformation slows down and continues to increase to the first peak at around 1.5 ms for 0.61 m clay. After a small rebound, the clay indent continues to increase to its peak after 2 ms when the deformation in the clay slows down to reach a plateau. Due to the confinement from the PVC pipe, the 0.15 m clay starts to rebound at an earlier time, ~1 ms. The residual clay indents in the 0.15 m block were about 10-15% smaller compared to the dynamic peak.

It can be seen from the simulations that the residual clay indents do not always correspond to the peak clay indents, especially for smaller clay block. For 0.61 m clay block, the clay indents at around 3.5 ms are about same value as the corresponding peak values. For the 0.15 m clay block, the clay indents at 2 ms are about 15% less than the respective peak indents.

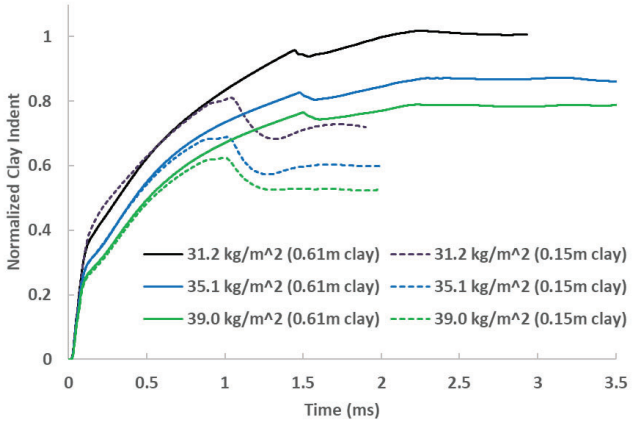

Figure 12 The comparison of clay indent time history between 0.61 m and 0.15 m clay block

Figure 13 shows the penetration at various times for armour areal density of 31.2 kg/m^2, 35.1 kg/m^2, 39.0 kg/m^2, with 0.61 m clay block cases. After impact, the projectile started to penetrate the ceramics. For 31.2 kg/m^2 and 35.1 kg/m^2 hard-armour, the projectile perforated the ceramics at around 50 μs, and 100 μs, respectively. But the projectile was arrested in the ceramics for 39.0 kg/m^2 armour and the composite failed partially right behind the ceramics where they were bonded together.

For all the cases, the projectile rotated either clockwise or counter-clockwise during the impact due to the non-symmetric deformation and failure of the ceramics, which validated the necessity of half model instead of quarter model. The failure of a brittle material like ceramic arises from its order of magnitude lower tensile strength than its compressive strength. As a result, crack appear in the hoop directions causing radial and cone cracks. Under perfectly axially symmetric impact and boundary conditions, a homogeneous target should break into infinite number of radial cracks when the hoop stress exceeds the tensile strength. However, this rarely happens in the experiments due to lack of perfect symmetry in the impact and boundary conditions, and also due to lack of homogeneity in the material causing cracks to preferentially appear at points of weak strength (defects, inclusions, voids, pre-existing micro-cracks, etc.) Cracks nucleating at such sites relieve the surrounding material of stress, leading to finite number of cracks in the target, and hence a non-symmetric crack pattern. While numerical simulations do not model such material heterogeneities explicitly, they do possess geometric asymmetry due to finite element mesh discretization and numerical approximations. While a full symmetry model is preferable to account for full penetrator-target interaction, it is computationally expensive. Therefore, a half symmetry model was employed to improve the numerical accuracy compared to a quarter-symmetry model while enabling a reasonable computation time for the calculations.

The clay initially deformed together with the shoot-pack. When the clay deformed faster than the shoot-pack, a gap was generated between them, at around 100 μs. Due to the gap, no further energy was transferred to the clay and the clay deformation slowed down, as shown in Figure 12. The slope of

https://doi.org/10.52202/078352-0038

the time history of clay indents changed suddenly around 100 μs due to the separation of clay and shoot-pack.

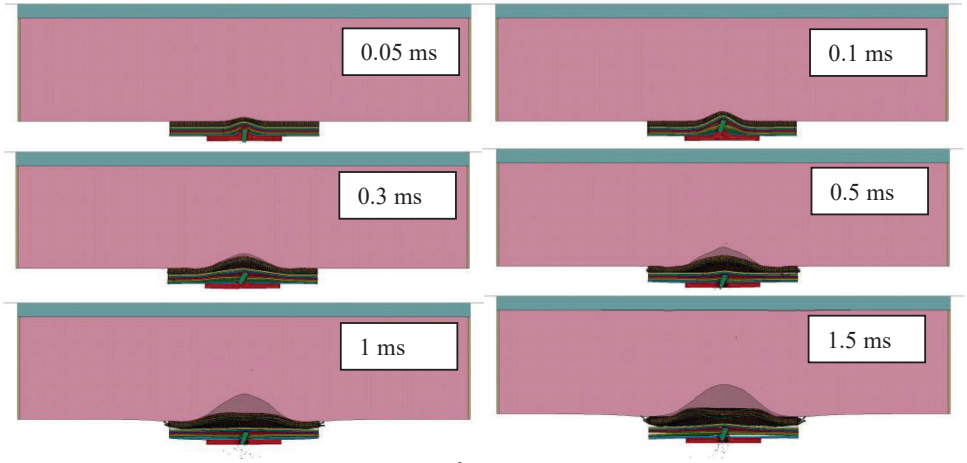

(a) 31.2 kg/m^2, 0.61 m clay block

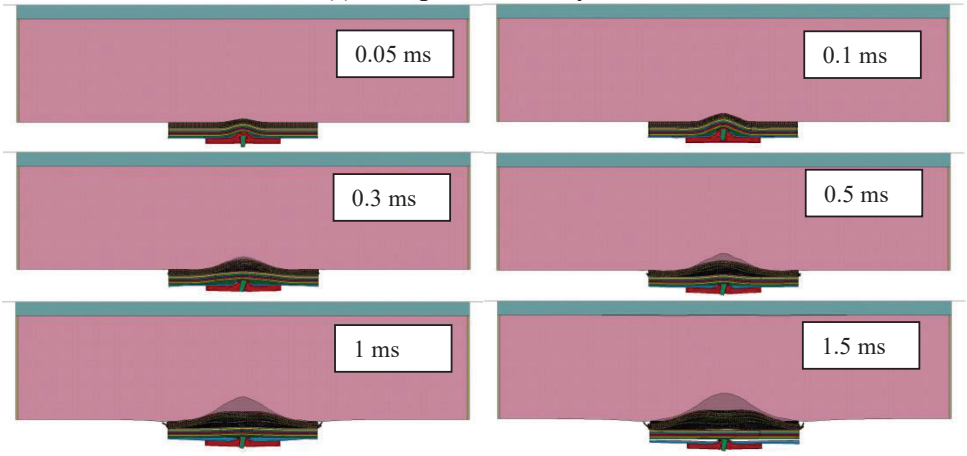

(b) 35.1 kg/m^2, 0.61 m clay block

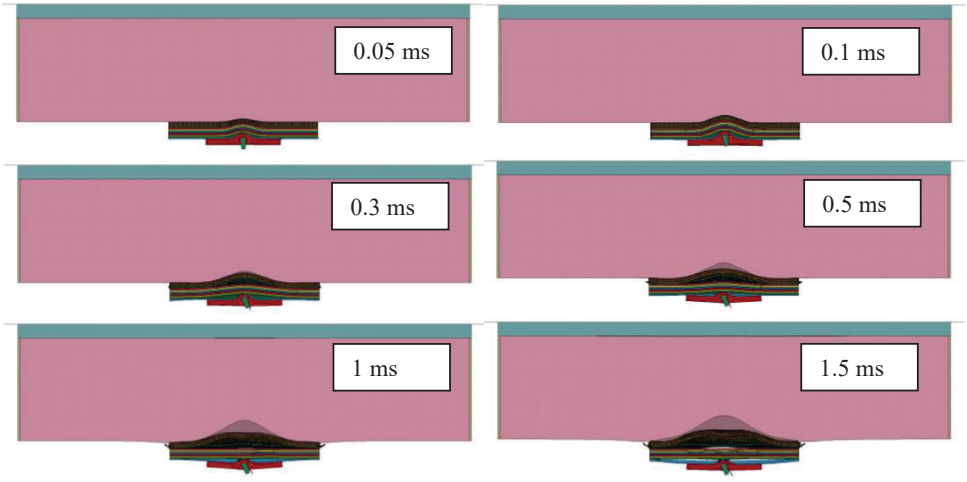

(c) 39.0 kg/m^2, 0.61 m clay block

Figure 13 The penetration at various time for armour areal densities of (a) 31.2 kg/m^2, (b) 35.1 kg/m^2, and (c) 39.0 kg/m^2, and 0.61 m wide clay block

https://doi.org/10.52202/078352-0038

Figure 14 shows the penetration at various time for armour areal density of 39.0 kg/m^2 with 0.15 m diameter clay block. Compared to Figure 13(c), due to the smaller size in radius, the clay deformation was confined by the PVC pipe, resulting in a smaller clay indent.

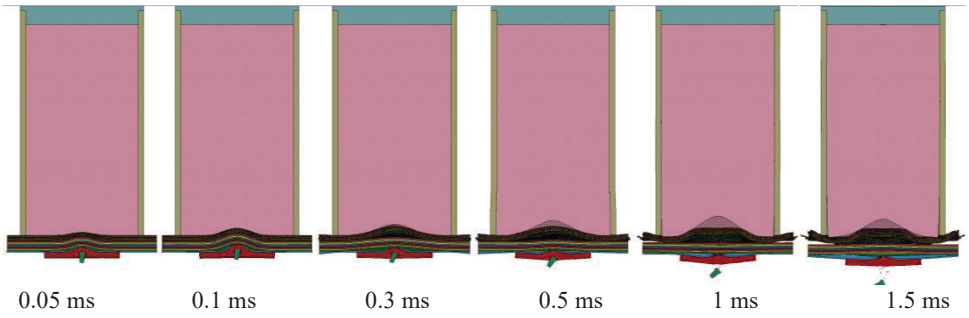

Figure 14 The penetration at various time for 39.0 kg/m^2, 0.15 m diameter clay block

Figure 15 shows the pressure contours in both 0.61 m and 0.15 m clay blocks for various times. The pressure wave propagated in a "spherical" direction towards the edge of the clay. As the pressure wave propagates, its amplitude decreases. The pressure wave, reflected from the end of the clay confined by the plywood, arrived at the impact region at around 1.5 ms, when the clay indent started to rebound, as shown in Figure 12. Similarly in the smaller clay block, the pressure wave arrived at the side earlier and the reflected pressure wave returned to the impact region at around 1 ms. The rebound in the 0.15 m clay was larger probably due to the smaller PVC pipe and stronger reflected pressure wave.

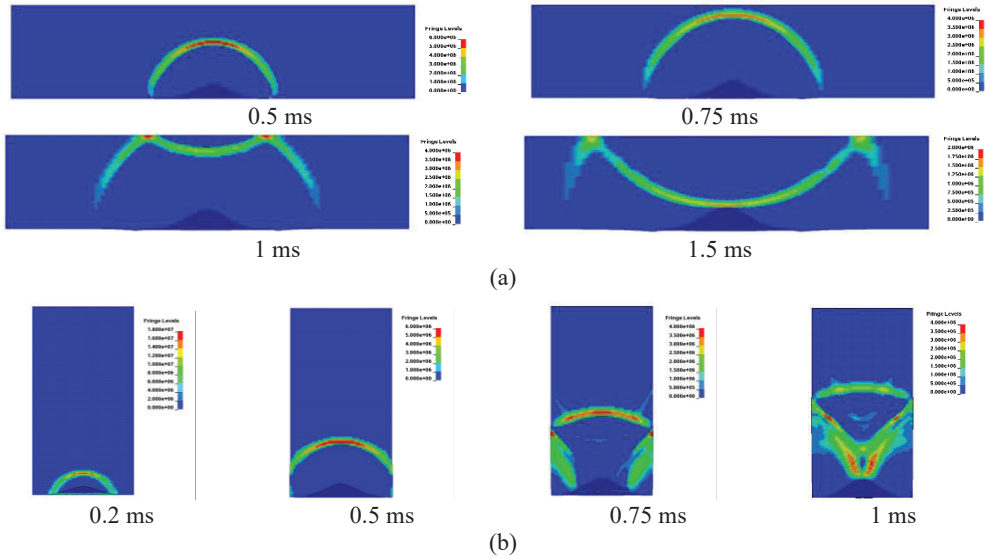

Figure 15 The pressure contour in the (a) 0.61 m, and (b) 0.15 m clay block

Table 1 lists the normalized residual clay indents and standard deviations of test data, predicted peak clay indents and clay indents at computation termination time. The measured residual clay indents were about 30% less in the 0.15 m clay block than in the 0.61 m clay block. The clay indents at computation termination time of the model agree very well with the residual clay indents measured in the experiments. The rebound was calculated by the indents at termination time and peak indents. The clay rebound was up to 15% in 0.15 m clay.

https://doi.org/10.52202/078352-0038

Table 1 Comparison between test and model

Clay size (m)	Hard armour areal density (kg/m^2)	Normalized clay indents				
		Test		Model		
		Average	Standard deviation	Peak	Indents at termination time	Rebound
0.15	31.2	0.73	0.069	0.81	0.72	11.1%
	35.1	0.63	0.029	0.69	0.60	13.0%
	39.0	0.56	0.044	0.62	0.53	14.5%
0.61	31.2	0.96	0.039	1.02	1.01	1.0%
	35.1	0.88	0.015	0.87	0.86	1.2%
	39.0	0.84	0.011	0.79	0.79	0.0%

6. CONCLUSION

In this work, ballistic impact tests were conducted to measure the residual indents in the clay blocks for three different thicknesses of hard-armour with a shoot-pack between the hard-armour and clay block. To understand the effect of boundary conditions, two different sizes of clay blocks were used in the experiments: a 0.61 m × 0.61 m × 0.14 m rectangular clay block and a 0.15 m diameter × 0.28 m thick cylindrical clay block. The test data showed that the residual clay indents decreased with increased thickness of hard-armour, as expected. The residual clay indents were about 30% less in the 0.15 m cylindrical clay block than in the 0.61 m rectangular clay block, which was mainly due to the smaller clay size and confinement effects of the PVC pipe.

A numerical model was developed to capture the interactions between hard-armour, shoot-pack and clay block. The material models for the composite, shoot-pack and clay were calibrated with impact test data in our earlier studies. The simulations using the calibrated clay model captured the rebound in the clay.

The simulations showed that the clay indents increased rapidly together with the deformed shoot-pack and then slowed down when a gap formed between the shoot-pack and clay, and hence no further energy was transferred to the clay. The clay continued to deform until the reflected wave from the rear surface arrived, when the clay started to rebound. The rebound depended on the clay size. For the smaller 0.15 m clay, the clay rebounded much earlier and the magnitude of rebound was about 15%. The clay had a very small rebound at a later time in the 0.61 m clay block. The predicted clay indents agreed reasonably well with the tested values of residual clay indents.

Since the dynamic clay indent is higher than the residual clay indent, the former appears to be a better metric to use to characterize armour performance and relate it to potential behind armour blunt trauma. However, it is not always feasible to measure the dynamic indentation in experiments using radiographic methods due to opacity of large targets to x-ray. Therefore, a modelling approach outlined in this study can be used to correlate the peak dynamic clay indent to the residual clay indent. Other parameters of interest, such as, stress, strain, energy and momentum transfer from the projectile to the clay can also be quantified from the simulation.

References

[1] M.J. Van der Jagt-Deutekom, Dr. E.P. Carton, M.M.G.M. Philipens, Separation phenomena between armour plate and clay backing during projectile impact, TNO report R10755, 2012.

[2] Timothy G. Zhang, Juliana Ivancik, Randy A Mrozek, Sikhanda S. Satapathy, Material Characterization of Ballistic Roma Plastilina No. 1 Clay, 30th International Symposium On Ballistics, Long Beach, CA, Sept. 11-15, 2017.

[3] Mary J Graham, Timothy Zhang, Experimental Investigation of Geometric Effects on Ballistic Clay Backing Material, ARL-TR-8717, , U.S. Army Research Laboratory, Aberdeen Proving Ground, MD, June 2019.

[4] Zhang TG, Satapathy SS, Vargas-Gonzalez LR, Walsh SM. Modeling ballistic response of ultra-high-molecular-weight polyethylene (UHMWPE), ARL-TR-7723, U.S. Army Research Laboratory, Aberdeen Proving Ground, MD, 2016.

https://doi.org/10.52202/078352-0038

[5] Timothy G Zhang, Phillip A Jannotti, Sikhanda S Satapathy, Jason R Mcdonald, Brian E Schuster, Indent depth and volume in the clay backing for soft and hard armour, Proceedings of Personal Armour Systems Symposium 2018, Washington, DC, Oct. 1-5, 2018.
[6] D.S. Cronin, K. Bui, C. Kaufmann, G. McIntosh, and T. Berstad, "Implementation and validation of the Johnson-Holmquist ceramic material model in LS-Dyna", Proc. 4th Eur. LS-DYNA Users Conf. 1, 47-60 (2003).
[7] G. R. Johnson, S. R. Beissel, C. A. Gerlach, T. J. Holmquist, User instruction for the 2018 version of EPIC, Southwest Research Institute, Sept. 2018.

https://doi.org/10.52202/078352-0038